



ELSEVIER

Contents lists available at ScienceDirect

## Journal of Solid State Chemistry

journal homepage: [www.elsevier.com/locate/jssc](http://www.elsevier.com/locate/jssc)

# Crystal structure of $\text{LiLnW}_2\text{O}_8$ ( $\text{Ln} = \text{lanthanides and Y}$ ): An X-ray powder diffraction study

J.M. Postema, W.T. Fu\*, D.J.W. IJdo

Leiden Institute of Chemistry, Gorlaeus Laboratories, Leiden University, P.O. Box 9502, 2300 RA Leiden, The Netherlands

## ARTICLE INFO

## Article history:

Received 16 March 2011

Received in revised form

27 May 2011

Accepted 29 May 2011

Available online 7 June 2011

## Keywords:

Crystal structure and symmetry

X-ray diffraction

Phase transition

Double tungstates

## ABSTRACT

Crystal structures that occur in  $\text{LiLnW}_2\text{O}_8$  ( $\text{Ln} = \text{lanthanides and Y}$ ) have been studied using Rietveld profile analysis of X-ray diffraction data. Two types of structures were observed. The scheelite structure of the space group  $I4_1/a$  is adopted for compounds containing large lanthanides  $\text{Ln} = \text{La–Gd}$ . For smaller lanthanides ( $\text{Ln} = \text{Dy–Lu and Y}$ ) the wolframite structure with the space group  $P2/n$  is observed. In  $\text{LiTbW}_2\text{O}_8$ , both structures occur. The phase transition between the two is a slow process making the obtainment of pure low temperature phase (wolframite) difficult. The space groups  $P\bar{1}$  and  $P2$ , recently reported for  $\text{LiEuW}_2\text{O}_8$  and  $\text{LiYW}_2\text{O}_8$ , have not been observed in this series of compounds.

© 2011 Elsevier Inc. All rights reserved.

## 1. Introduction

Most divalent metal ion tungstates  $\text{AWO}_4$  belong to either the scheelite structure ( $A = \text{Ba, Sr, Ca, Pb}$ ) or the wolframite structure ( $A = \text{Mn, Fe, Co, Ni, Zn, Cd}$ ). The scheelite structure is a superstructure of fluorite. The oxygen atoms are in a distorted simple cubic arrangement; the  $A$ -cations have eight coordination of oxygen and  $W$  coordinates with only four oxygens. In the wolframite structure, the oxygen atoms are in a nearly hexagonal closed packing; both  $A$  and  $W$  are in octahedral oxygen coordination. In  $\text{AWO}_4$  the substitution of  $2A^{2+}$  into  $A^+$  and  $A^{3+}$  is well known. Klevtsov and Kletsova [1] reported the polymorphism of a large number of double molybdates and tungstates with the formula  $A^+A^{3+}(\text{MO}_4)_2$ , where  $A^+ = \text{Li–Cs, Ag and Tl}^+$ ,  $A^{3+} = \text{lanthanides, Y, Bi, In, Sc, Ga, Fe, Cr and M} = \text{Mo or W}$ . Approximately 30 different structural types were identified. The crystal structures of the most common types have been determined, but the structural details of many compounds remain up to now unknown.

The double tungstates  $\text{LiLnW}_2\text{O}_8$  ( $\text{Ln} = \text{lanthanides and Y}$ ) have long been known and were reported to adopt either the scheelite structure or wolframite-like structure depending on the size of  $\text{Ln}$  as well as on temperature. Klevtsov and Kletsova reported the structure diagram for  $\text{LiLnW}_2\text{O}_8$  [1]. According to this diagram, the compounds with  $\text{Ln} = \text{La–Gd}$  have the scheelite structure at high temperature and the  $\alpha$ - $\text{LiPrW}_2\text{O}_8$  structure at low temperature, respectively. The later structure consists of  $\text{W}_4\text{O}_{16}$  unit of four edge-shared  $\text{WO}_6$  octahedra forming sheets parallel to the

$[101]$  direction with the large cations being located between the sheets in an ordered fashion. However, no transition temperatures were defined between the two structures. For  $\text{Ln} = \text{Tb–Lu}$  including  $\text{Y}$ , the compounds adopt either the wolframite structure (i.e.  $\beta$ - $\text{LiYbW}_2\text{O}_8$  with space group  $P2/n$ ) at high temperature or the  $\text{NaNW}_2\text{O}_8$  structure (space group  $P2/c$ ) at low temperature, respectively. Again, no transition temperatures were yet given. Besides these earlier works, Huang et al. have reported the crystallographic data of the scheelite-like  $\text{LiNdW}_2\text{O}_8$  based on single crystal diffraction data [2].

The luminescence properties of  $\text{AEuM}_2\text{O}_8$  ( $A = \text{alkali metal and M} = \text{W and Mo}$ ) have been previously reported by van Vliet and Blasse [3]. Some of these double tungstates and/or molybdates have received renewed interests in recent years. In particular, several studies have pointed out that  $\text{LiEu}(\text{W,Mo})_2\text{O}_8$  are efficient red-emitting phosphors with excitation in the near-UV and blue region being suitable for fabrication of white LEDs [4–9]. Although most authors described the crystal structure of these compounds as tetragonal scheelite [3–5,8,9], the structural details have not been reported. Recently, Chiu et al. have studied the structural and photoluminescence properties of  $\text{LiEuW}_{2-x}\text{Mo}_x\text{O}_8$  [6,7]. They reported that this series of compounds is isostructural to  $\text{KEuMo}_2\text{O}_8$  [10] having triclinic symmetry. They also refined, using the Rietveld method and X-ray powder diffraction data, the atomic positions of the two end-members in the space group  $P\bar{1}$ . Doubt is, however, cast on their choice of the structural model. First, Chiu et al. did not show any evidence that the symmetry of  $\text{LiEuW}_2\text{O}_8$  and  $\text{LiEuMo}_2\text{O}_8$  is truly triclinic. Second, the structure model of  $\text{KEuMo}_2\text{O}_8$  describes an ordered arrangement of large cations. In their refinements of  $\text{LiEuW}_2\text{O}_8$  and  $\text{LiEuMo}_2\text{O}_8$  these ions are randomly distributed in two crystallographically

\* Corresponding author. Fax: +31 71 5274537.

E-mail address: [w.fu@chem.leidenuniv.nl](mailto:w.fu@chem.leidenuniv.nl) (W.T. Fu).

different sites without giving the underlying reason. Third, the refined atomic positions are listed, as supplementary information, without the standard deviations. Last but not least, the  $\text{WO}_4$  tetrahedra in  $\text{LiEu}(\text{W},\text{Mo})_2\text{O}_8$  described in the space group  $P\bar{1}$  are highly asymmetric. Some of the W–O bond distances as well as the O–W–O angles are unrealistic suggesting that the triclinic space group may not be correct.

Besides this controversy, the space group reported for  $\text{LiLnW}_2\text{O}_8$  with smaller lanthanides differs too. Klevtsova and Belov reported the space group  $P2/n$  for wolframite-like  $\text{LiYbW}_2\text{O}_8$  [11]. Kim et al. have lately investigated the low temperature cofiring ceramic properties of the  $\text{LiLnW}_2\text{O}_8$ – $\text{BaWO}_4$  system and described the structure of the model compound  $\text{LiYW}_2\text{O}_8$  in the space group  $P2$  [12]. To clear the literature conflicts on double tungstates, we carried out a systematic X-ray powder diffraction study on the crystal structure of  $\text{LiLnW}_2\text{O}_8$  ( $Ln$ =Lanthanides and Y). In this paper, we show that the correct space groups of  $\text{LiLnW}_2\text{O}_8$  are  $I4_1/a$  and  $P2/n$ , respectively. No evidences have ever been found that the title compounds adopt the triclinic  $P\bar{1}$  or the monoclinic  $P2$  space groups.

## 2. Experimental

Samples of  $\text{LiLnW}_2\text{O}_8$  were prepared from  $\text{Li}_2\text{CO}_3$  (Noury-Baker N.V., 99.9%),  $\text{Ln}_2\text{O}_3$  (Elcomat-Lmf 99.9% except  $\text{Eu}_2\text{O}_3$  Acros Organics 99.9%),  $\text{Y}_2\text{O}_3$  (Acros Organics 99.9%),  $\text{Pr}_6\text{O}_{11}$  (Elcomat-Lmf 99.9%),  $\text{Tb}_4\text{O}_7$  (Alfa Aesar 99.99%) and  $\text{WO}_3$  (Alfa Aesar 99.8%) in alumina crucibles using the standard solid state reaction. The stoichiometric mixtures, corresponding to about 1 g of final product, were thoroughly ground in agate mortar with pestle by adding a small amount of ethanol. The mixtures were first heated at 1073 K for 4 h and subsequently quenched. After regrinding they were sintered at the same temperature overnight (~15 h) and were furnace cooled to room temperature in about 10 h. All syntheses were carried out in air. For preparation of  $\text{LiYW}_2\text{O}_8$ , 5 mol%  $\text{Li}_2\text{CO}_3$  was used in excess in order to obtain the pure phase.

X-ray powder diffraction data were collected on a Philips X'Pert diffractometer, equipped with the X'Celerator, using  $\text{CuK}\alpha$  radiations in steps of  $0.02^\circ$  ( $2\theta$ ) and 10 s counting time in the  $2\theta$ -range between  $10^\circ$  and  $140^\circ$ . The calculations were performed by the Rietveld method using the Rietica computer programme [13]. The Chebishev-polynomial function with 12 parameters was used to fit the background. The profiles were described by a Pseudo-Voigt function.

## 3. Results

The X-ray diffraction of  $\text{LiLnW}_2\text{O}_8$  shows two types of patterns (Fig. 1) indicating that they adopt different crystal structures. The first type includes the compounds with  $Ln$ =La–Tb,<sup>1</sup> and the second type comprises those with  $Ln$ =Dy–Lu and Y, which is in rough agreement with the earlier observation of Klevtsov and Klevtsova [1].

The diffraction patterns of the first group resemble the simple scheelite and all diffraction lines can be indexed in a tetragonal cell with the cell dimension of  $a \approx 5.3 \text{ \AA}$  and  $c \approx 11.4 \text{ \AA}$  using the space group  $I4_1/a$  (see e.g. PDF cart 88-0854). Careful examinations of profiles showed no evidences of either lower symmetry or possible ordering of Li and  $Ln$  cations. Consequently, the initial structure model adopted for these compounds is the scheelite  $\text{CaWO}_4$  with space group  $I4_1/a$  [14], and the large Li and  $Ln$  cations are randomly distributed. The Rietveld refinements using X-ray diffraction data converged smoothly, and yielded satisfactory results. To justify the choice of the tetragonal model, we also

<sup>1</sup>  $\text{LiTbW}_2\text{O}_8$  may adopt both structures depending on the thermal history of the compound (see details in Section 4).

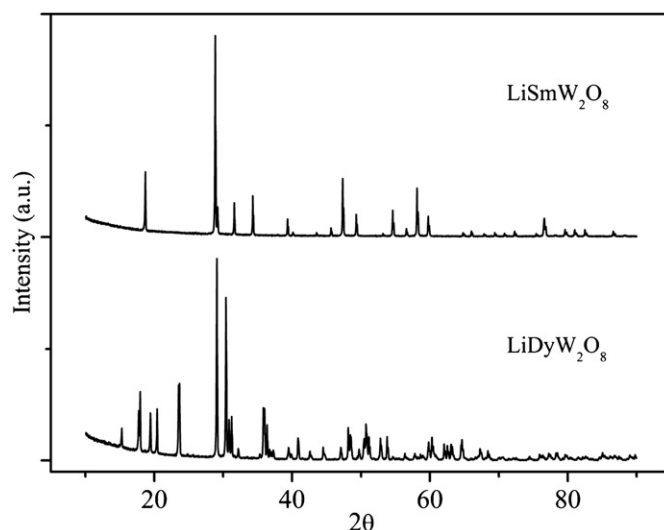


Fig. 1. Part of the X-ray diffraction patterns of  $\text{LiSmW}_2\text{O}_8$  and  $\text{LiDyW}_2\text{O}_8$  representing two structure types in  $\text{LiLnW}_2\text{O}_8$  with  $Ln$ =La–Tb and  $Ln$ =Dy–Lu and Y, respectively.

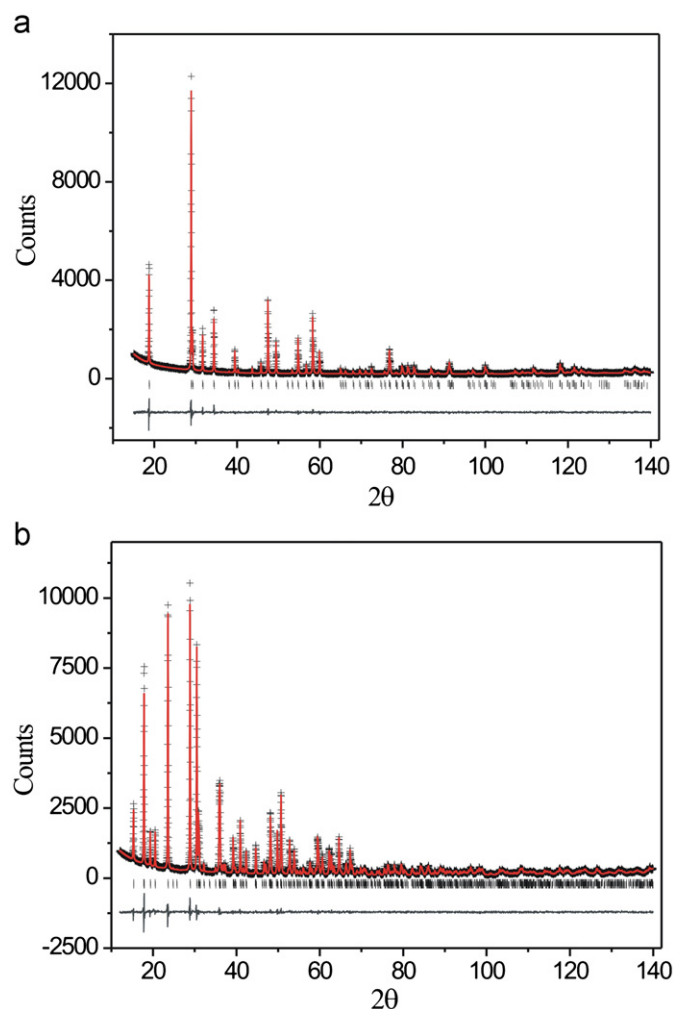


Fig. 2. Observed (crosses) and calculated (full line) profiles of the X-ray powder diffraction pattern for (a)  $\text{LiEuW}_2\text{O}_8$  and (b)  $\text{LiYW}_2\text{O}_8$  in the space group  $I4_1/a$  and  $P2/n$ , respectively. Tick marks indicate the positions of Bragg's reflections. Difference curves (observed—calculated) are shown at the bottom of each plot.

refined, in the case of  $\text{LiEuW}_2\text{O}_8$ , the model proposed by Chiu et al. [6,7]. The refinement in the triclinic space group  $P\bar{1}$  was found to be quite unstable; full convergence could only be

achieved using very high damping factors. Although a slightly lower agreement factor,  $R_{wp}=6.79\%$  in  $P\bar{1}$  vs.  $R_{wp}=6.86\%$  in  $I4_1/a$ , was obtained, such an improvement is not significant at all, since the  $P\bar{1}$  model has 37 more refinable parameters than the  $I4_1/a$  model. Considering further that the refined oxygen positions in  $P\bar{1}$  show very high standard deviations (roughly 10–20 times higher than the refined value in  $I4_1/a$ ), we concluded that the triclinic model is not compatible with the structure of  $LiLnW_2O_8$  ( $Ln=La-Tb$ ) (see also Section 4).

For the compounds  $LiLnW_2O_8$  with smaller lanthanide and Y, the X-ray diffraction patterns are obviously more complicated (Fig. 1), but all diffraction lines could be described with a monoclinic cell. Since there are two space groups reported thus far [11,12], comparison

refinements were carried out using the X-ray diffraction data of  $LiYW_2O_8$  in both models. The refinements in the space group  $P2/n$  [11] went quite readily, and yielded adequate fit between the experimental and calculated data. In the case of the space group  $P2$ , the original occupancy factors of two Li were reported by Kim et al. to be 1.22(10) and 0.74(10), respectively [12]. Since the value larger than unity is physically meaningless, they are fixed to 1 in our calculation. The refinement yielded similar fit with a slightly lower  $R_{wp}$ : 7.45% in  $P2$  vs. 7.80% in  $P2/n$ . However, with 16 more variables in  $P2$ , such an improvement is, again, insignificant. Inspection of the refined parameters also showed incompatibility of this model. For example, the refined  $y$ -coordinates of all atoms, e.g.  $y_{W(1)}=0.311(39)$  and  $y_{W(2)}=0.946(39)$ , have unusually high standard deviations

**Table 1**  
Refined crystallographic data of  $LiLnW_2O_8$  at room temperature.

Ln S.G.	La $I4_1/a$	Nd	Sm	Eu	Gd	Tb <sup>a</sup>
$a$ (Å)	5.32536(5)	5.25956(5)	5.22637(4)	5.21198(6)	5.19904(5)	5.18468(5)
$c$ (Å)	11.5983(1)	11.4083(1)	11.3194(1)	11.2886(1)	11.2537(1)	11.2235(1)
Li/ $Ln^b$ (4a)	(0,1/4,1/8)	(0,1/4,1/8)	(0,1/4,1/8)	(0,1/4,1/8)	(0,1/4,1/8)	(0,1/4,1/8)
W (4b)	(1/2,3/4,1/8)	(1/2,3/4,1/8)	(1/2,3/4,1/8)	(1/2,3/4,1/8)	(1/2,3/4,1/8)	(1/2,3/4,1/8)
O (16f)	(x,y,z)	(x,y,z)	(x,y,z)	(x,y,z)	(x,y,z)	(x,y,z)
$x$	0.7332(11)	0.7527(9)	0.7565(8)	0.7476(8)	0.7500(7)	0.7524(8)
$y$	0.57734(13)	0.5940(10)	0.5949(9)	0.5937(9)	0.5914(8)	0.5877(10)
$z$	0.0447(5)	0.0382(4)	0.0401(4)	0.0374(4)	0.0372(3)	0.0384(4)
$B$ (Å <sup>2</sup> ) <sup>c</sup>	0.22(2)	0.32(2)	0.30(2)	0.43(2)	0.71(2)	0.49(2)
$R_{wp}$ (%)	12.28	8.61	7.79	6.86	6.13	7.03
$R_p$ (%)	9.05	6.69	5.00	5.27	4.72	5.34
$\chi^2$	2.85	1.73	1.83	1.72	1.75	2.21
Ln S.G.	Dy $P2/n$	Ho	Er	Yb	Lu	y
$a$ (Å)	10.0409(2)	10.0017(1)	9.9632(1)	9.8890(1)	9.8525(1)	9.9932(1)
$b$ (Å)	5.79404(9)	5.79143(7)	5.78567(6)	5.79035(8)	5.79307(7)	5.79743(7)
$c$ (Å)	5.01216(8)	5.00734(7)	5.00354(5)	4.99227(7)	4.98626(6)	5.00639 (7)
$\beta$ (deg)	94.5869(9)	94.3372(7)	94.0804(6)	93.4257(8)	93.1220(8)	94.1992(8)
Li (2f)	(1/4,y,3/4)	(1/4,y,3/4)	(1/4,y,3/4)	(1/4,y,3/4)	(1/4,y,3/4)	(1/4,y,3/4)
$y$	0.230(8)	0.217(6)	0.236(6)	0.261(6)	0.247(6)	0.230(5)
$Ln$ (2e)	(1/4,y,1/4)	(1/4,y,1/4)	(1/4,y,1/4)	(1/4,y,1/4)	(1/4,y,1/4)	(1/4,y,1/4)
$y$	0.7010(3)	0.6997(3)	0.6980(2)	0.6940(2)	0.6916(2)	0.6978(3)
W (4g)	(x,y,z)	(x,y,z)	(x,y,z)	(x,y,z)	(x,y,z)	(x,y,z)
$x$	0.0177(1)	0.01731(7)	0.01711(8)	0.01607(8)	0.01525(8)	0.0171(1)
$y$	0.1824(2)	0.1827(1)	0.1819(2)	0.1822(1)	0.1820(1)	0.1824(1)
$z$	0.2526(2)	0.2525(2)	0.2519(1)	0.2508(2)	0.2504(1)	0.2522(1)
O1 (4g)	(x,y,z)	(x,y,z)	(x,y,z)	(x,y,z)	(x,y,z)	(x,y,z)
$x$	0.108(1)	0.1119(8)	0.1154(9)	0.1192(9)	0.1161(9)	0.1136(8)
$y$	0.621(2)	0.621(1)	0.627(1)	0.622(1)	0.625(1)	0.620(1)
$z$	0.894(2)	0.894(1)	0.900(2)	0.896(2)	0.894(2)	0.889(1)
O2 (4g)	(x,y,z)	(x,y,z)	(x,y,z)	(x,y,z)	(x,y,z)	(x,y,z)
$x$	0.150(1)	0.1362(8)	0.1387(9)	0.1382(9)	0.1360(9)	0.1384(8)
$y$	0.377(2)	0.377(1)	0.378(1)	0.377(1)	0.383(1)	0.084(1)
$z$	0.437(2)	0.410(2)	0.417(2)	0.412(2)	0.411(2)	0.408(1)
O3 (4g)	(x,y,z)	(x,y,z)	(x,y,z)	(x,y,z)	(x,y,z)	(x,y,z)
$x$	0.116(1)	0.1137(8)	0.116(1)	0.1159(9)	0.1127(9)	0.1185(8)
$y$	0.082(2)	0.089(1)	0.087(1)	0.089(1)	0.095(1)	0.084(1)
$z$	0.960(2)	0.964(2)	0.959(2)	0.965(2)	0.962(2)	0.960(2)
O4 (4g)	(x,y,z)	(x,y,z)	(x,y,z)	(x,y,z)	(x,y,z)	(x,y,z)
$x$	0.098(1)	0.0960(8)	0.0967(9)	0.1067(9)	0.1023(9)	0.10245(8)
$y$	0.893(2)	0.890(1)	0.888(1)	0.895(1)	0.892(1)	0.892(1)
$z$	0.466(2)	0.456(1)	0.455(2)	0.457(2)	0.460(2)	0.457(2)
$B$ (Å <sup>2</sup> ) <sup>c</sup>	0.24(2)	0.31(2)	−0.01(2)	0.14(2)	0.12(2)	0.22(2)
$R_{wp}$ (%)	6.01	6.97	7.25	8.40	8.41	7.47
$R_p$ (%)	4.67	5.32	5.55	6.31	6.38	5.61
$\chi^2$	1.83	2.19	2.12	2.67	2.72	2.08

<sup>a</sup> Diffraction data was taken on the normally cooled sample.

<sup>b</sup> Li and Ln are randomly distributed.

<sup>c</sup> An overall thermal parameter was used in the refinements.

indicating that the atomic positions described in  $P2$ , i.e.  $(x,y,z)$  and  $(\bar{x},y,\bar{z})$ , are not consistent with the structure. In addition, the refined  $x$ - and  $z$ -coordinates of the two W atoms readily, i.e.  $x_{W(1)}=0.2351(5)$ ,  $z_{W(1)}=0.4980(12)$  and  $x_{W(2)}=0.7306(5)$ ,  $z_{W(2)}=-0.0028(11)$ , show obviously an  $n$ -glide plane perpendicular to the  $b$ -axis. In fact, the correlation matrix reveals that all pairs of atoms are strongly correlated. For those reasons, the space group  $P2$  was discarded from further consideration.

**Table 2**  
Interatomic distances in some representative  $\text{LiLnW}_2\text{O}_8$ .

$Ln$	Nd	Eu		Dy	Y
W–O	1.849(4) × 4	1.826(4) × 4	W–O1	1.81(1)	1.840(7)
			W–O2	1.92(1)	1.798(8)
			W–O3	1.92(1)	1.924(8)
			W–O4	2.25(1)	2.268(8)
Li/ $Ln$ –O	2.415(5) × 4 2.438(5) × 4	2.397(4) × 4 2.423(4) × 4	Li–O1	2.80(4) × 2	2.75(2) × 2
			Li–O2	1.98(2) × 2	2.16(1) × 2
			Li–O3	1.96(2) × 2	1.94(1) × 2
			Li–O4	2.79(3) × 2	2.80(2) × 2
			$Ln$ –O1	2.23(1) × 2	2.231(8) × 2
			$Ln$ –O2	2.36(1) × 2	2.328(8) × 2
			$Ln$ –O3	2.91(1) × 2	2.928(8) × 2
			$Ln$ –O4	2.23(1) × 2	2.178(7) × 2

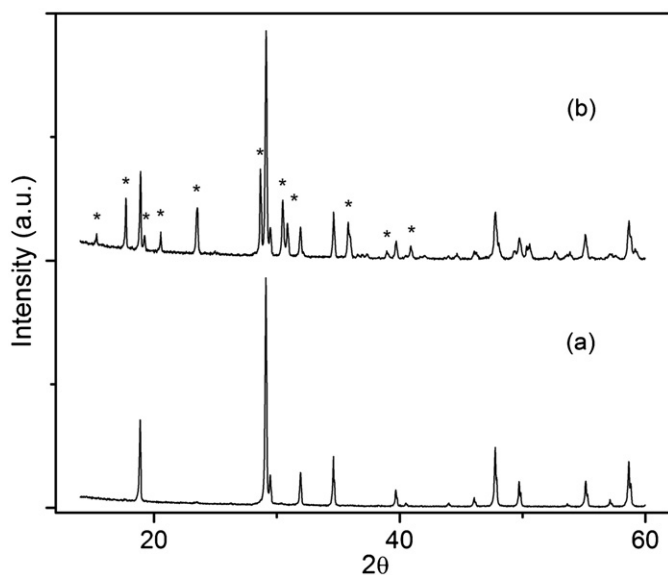


**Fig. 3.** Portion of the X-ray powder diffraction patterns of  $\text{LiTbW}_2\text{O}_8$  showing (a) The sample obtained by furnace cooling from high temperature and (b) sample kept at 600 °C overnight and followed by furnace cooling (3 times). In (b) some reflections belonging to the wolframite phase are indicated by asterisks.

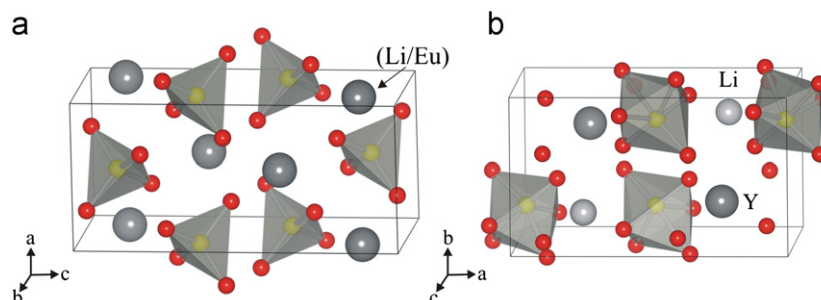


**Fig. 4.** Schematic representation of the crystal structure of  $\text{LiEuW}_2\text{O}_8$  (a) and  $\text{LiYW}_2\text{O}_8$  (b). Note that the large cations are random in scheelite (a) but are ordered in wolframite (b). The  $\text{WO}_4$  tetrahedra and  $\text{WO}_6$  octahedra are also shown.

The structure of  $\text{LiLnW}_2\text{O}_8$  were described in the space groups  $I4_1/a$  and  $P2/n$  for  $Ln=\text{La–Tb}$  and  $Ln=\text{Dy–Lu}$  and  $Y$ , respectively. Fig. 2 shows the plots of the observed and calculated X-ray profiles of two representatives of  $\text{LiLnW}_2\text{O}_8$ . The refined lattice parameters, atomic positions and interatomic distances are given in Tables 1 and 2, respectively.

#### 4. Discussion

The present investigation shows that  $\text{LiLnW}_2\text{O}_8$  adopts, at room temperature, either the tetragonal scheelite or the monoclinic wolframite structure depending on the size of  $Ln$ . Our results confirm essentially the earlier findings of Klevtsov and Klevtsova [1], except for a few minor differences. For example,  $\text{LiTbW}_2\text{O}_8$  lies, according to the diagram, in the same structure group of  $\beta\text{-LiYbW}_2\text{O}_8$ . We found, however, that it adopts easily the scheelite structure if the sample is normally cooled in furnace. For this sample only a trace of the wolframite phase could be seen with the intensity maximum not exceeding 1% of the strongest reflection of the scheelite phase (Fig. 3(a)). On the other hand, the amount of the wolframite phase increases when  $\text{LiTbW}_2\text{O}_8$  was kept at 600 °C overnight followed by furnace cooling to room temperature. Nevertheless, the scheelite  $\rightarrow$  wolframite phase transition is rather slow; the scheelite remains as majority phase even after three cycles of the low temperature treatment (Fig. 3(b)). Clearly, for  $\text{LiTbW}_2\text{O}_8$  the wolframite structure is thermodynamically more stable at low temperature, but the sluggish phase transition makes the obtaining of pure wolframite phase difficult. Another difference is that the “low temperature”  $\alpha\text{-LiPrW}_2\text{O}_8$  structure reported for the compounds with  $Ln=\text{La–Sm}$  [1] has not been observed. However, we noted that Klevtsova et al. observed this structure from their single crystal experiment; the crystals had been prepared at temperatures between 400 and 600 °C by applying high pressure (700–1500 atm) and using  $\text{LiCl}$  as flux [15]. Evidently,  $\alpha\text{-LiPrW}_2\text{O}_8$  is either only stable under those crystal growth conditions or the polymorphic phase transformation from the scheelite to  $\alpha\text{-LiPrW}_2\text{O}_8$  is controlled by kinetics, which does not occur by furnace cooling of the powder samples in our investigation.

The scheelite structure belongs to tetragonal class ( $I4_1/a$ ) consisting of isolated  $\text{WO}_4^{2-}$  tetrahedral unit. The larger Li and  $Ln$  cations are random and are surrounded by eight oxygen ions arranged in a highly deformed cube (Fig. 4(a)). In scheelite the oxygens are not close packed, but the structure can be derived from the fluorite structure with Li/ $Ln$  in eight coordination and W in tetrahedral coordination. On the other hand, the wolframite structure is a more closely packed structure, which can be viewed as a slightly deformed hexagonal packing of oxygens with the Li/ $Ln$  and W ions occupying half of the octahedral sites of the alternate layers. Unlike the scheelite, all metals ions in double wolframites are octahedrally coordinated with the oxygen anions (Fig. 4(b)). In addition, Li and  $Ln$

are ordered within the metal layer and the adjacent  $\text{LiO}_6$  and  $\text{LnO}_6$  octahedra share the common edge forming one dimensional chain parallel to the *c*-axis.

Another structure type, i.e.  $\text{NaNW}_2\text{O}_8$  [16], has also been reported by Klevtsov and Klevtsova for double wolframites  $\text{LiLnW}_2\text{O}_8$  with smaller *Ln* at low temperature [1]. The structure has the space group  $P2/c$  and consists of similar hexagonal packing of oxygens. However, the cation layers are different having the sequence of Li–W–Ln–W. We did not observe this type of structure in  $\text{LiLnW}_2\text{O}_8$  using the preparation methods described above.

As was mentioned earlier, the triclinic model proposed by Chiu et al. is not compatible with the double tungstates  $\text{LiLnW}_2\text{O}_8$  (*Ln*=La–Tb). The X-ray diffraction patterns of these compounds are typical of a tetragonal scheelite. Since the ionic radius of  $\text{Li}^+$  (0.92 Å for eight coordination) is significantly smaller than that of  $\text{K}^+$  (1.51 Å) [17], it does not seem to be logical to select the structure of  $\text{KEuMo}_2\text{O}_8$  for modelling  $\text{LiLnW}_2\text{O}_8$ . In fact, the structure described in the space group  $P\bar{1}$  shows some unrealistic bond distances and angles [6]. For example, the W1–O4 and W2–O5 bond lengths are either too long (2.280 Å) or too short (1.593 Å) as compared with the one refined in the scheelite structure (1.818(4) Å). It is also seen that the O–W–O angles of W(2)O4 tetrahedron vary from 74.38° to 136.90° being far different than the ideal value (109.47°). Clearly, the space group  $P\bar{1}$  fails to describe the double tungstates containing Li.

Kim et al. reported a different space group for  $\text{LiYW}_2\text{O}_8$  [12]. They came to this conclusion because they could not refine the structure in the space group  $P2/n$ . They fitted, therefore, the neutron diffraction data using several trial models and concluded that the space group  $P2$  is compatible with the structure. Although the fit they show may seem reasonable, there is some doubt about the validity of this model. For example, Kim et al. did not provide real evidence to justify their choice of the space group. In fact, the calculated neutron diffraction pattern using their model shows negligible intensities of the *h0l*-type reflections with  $h+l=2n+1$ . In addition, the reported site occupancy values for Li1 (1.22) and Li2 (0.74) cannot be correct. Although the authors argued that the possible disorder between Li and Y might be responsible for the abnormally large positive and negative thermal parameters of the two Li, such a possibility has not been examined in their refinement. It is unclear why Kim et al. failed to refine the structure in the space group  $P2/n$ . On the other hand, our Rietveld refinements of  $\text{LiLnW}_2\text{O}_8$  (*Ln*=Dy–Lu and Y) using X-ray diffraction data all went just smoothly and resulted in satisfactory fit.

It should be noticed that the recent investigations of double tungstates and molybdates focused mainly on their luminescence properties. In particular, the Eu-doped materials have been universally described as efficient red-emitting phosphors for near-UV or blue LED-chips [4–9]. Doubts are, however, cast on such a statement. Firstly, the excitation in the near-UV (~395 nm) or blue region (~465 nm) in these materials relays on the internal 4f–4f transitions, which are generally weak due to the parity selection rule. Indeed, from the diffuse reflectance spectra given in Ref. [6], the intensity of the intra-configurational

transitions is only a fraction of the allowed charge transfer band. This low absorption has put a serious question on whether those materials are suitable for the near-UV LED-based lamps. Secondly, the concentration quenching is a well-known phenomenon for lanthanides, which is due to energy migration among the identical luminescent centres and the subsequent energy loss at the proximity of quenching centres. For  $\text{Eu}^{3+}$ -activator, the exchange interaction between neighbouring Eu is believed to be effective if the Eu–Eu distance is shorter than about 5 Å [18]. In the scheelite structure, each large cation has four nearest neighbours forming thus zigzag chains along the [1 0 0] and [0 1 1]-directions. Considering the chemical formula  $\text{LiEuW}_2\text{O}_8$  and assuming a random distribution of large cations,  $\text{Eu}^{3+}$  will always find the closest neighbour(s) at the distance of 3.84 Å. Therefore, concentration quenching is expected to occur in Li containing double tungstates or molybdates. Indeed, our preliminary investigation of the  $\text{LiEu}_{1-x}\text{Y}_x\text{W}_2\text{O}_8$  system shows that under near-UV excitation the highest intensity of  $\text{Eu}^{3+}$ -emission occurs at  $x \approx 0.5$ . The detailed results will be published elsewhere.

In conclusion, we have synthesised  $\text{LiLnW}_2\text{O}_8$  (*Ln*=lanthanides and Y) and investigated their crystal structures at room temperature using X-ray powder diffraction data. Our results confirm essentially the earlier findings of Klevtsov and Klevtsova that these double tungstates adopt either the scheelite or the wolframite structure and the border of stability of the two structures lies at *Ln*=Tb.  $\text{LiTbW}_2\text{O}_8$  may adopt both structures at room temperature, although the scheelite structure is only stable at high temperature. In fact, due to a slow kinetics of the phase transition it is difficult to obtain low temperature wolframite phase in pure form for this compound. The recently reported triclinic space group  $P\bar{1}$  and the monoclinic space group  $P2$  for  $\text{LiEuW}_2\text{O}_8$  and  $\text{LiYW}_2\text{O}_8$ , respectively, have not been confirmed for any of these compounds.

## References

- [1] P.V. Klevtsov, R.F. Klevtsova, Zh. Strukt. Khimi 18 (1977) 419.
- [2] Xinyang Huang, Zhoubin Lin, Lizhen Zhang, Jiutong Chen, Guofu Wang, Cryst. Growth Des. 6 (2006) 2271.
- [3] J.P.M. van Vliet, G. Blasse, J. Solid State Chem. 76 (1988) 160.
- [4] Z.L. Wang, H.B. Liang, L.Y. Zhou, H. Wu, M.L. Gong, Q. Su, Chem. Phys. Lett. 412 (2005) 313.
- [5] J.G. Wang, X.P. Jing, C.H. Yan, J.H. Lin, F.H. Liao, J. Lumin. 121 (2006) 57.
- [6] C.H. Chiu, M.F. Wang, C.S. Lee, T.M. Chen, J. Solid State Chem. 180 (2007) 619.
- [7] C.H. Chiu, C.H. Liu, S.B. Huang, T.M. Chen, J. Electrochem. Soc. 154 (2007) j181.
- [8] K.S. Hwang, S. Hwangbo, J.T. Kin, Ceram. Int. 35 (2009) 2517.
- [9] X.H. He, M.Y. Guan, J.H. Sun, N. Liang, T.M. Shang, J. Mater. Sci. 45 (2010) 118.
- [10] R.F. Klevtsova, L.P. Koseeva, P.V. Klevtsov, Kristallografiya 19 (1974) 89.
- [11] R.F. Klevtsova, N.V. Belov, Kristallografiya 15 (1970) 43.
- [12] J.S. Kim, J.C. Lee, C.I. Cheon, H.J. Kang, Jpn. J. Appl. Phys. 45 (2006) 7397.
- [13] C.J. Howard, B.A. Hunter, A Computer Program for Rietveld Analysis of X-ray and Neutron Powder Diffraction Patterns, Lucas Heights Research Laboratories, 1998.
- [14] M.I. Kay, B.C. Frazer, I. Almodovar, J. Chem. Phys. 40 (1964) 504.
- [15] R.F. Klevtsova, L.Yu. Kharchenko, S.V. Borisov, V.A. Efremov, P.V. Klevtsov, Kristallografiya 24 (1979) 446.
- [16] P.V. Klevtsov, R.F. Klevtsova, J. Solid State Chem. 2 (1970) 278.
- [17] R.D. Shannon, Acta Crystallogr. A32 (1976) 751.
- [18] G. Blasse, B.C. Grabmeier, Luminescent Materials, first ed., Springer, Berlin, 1994.